Supplemental Materials

Quantifying the synergy of drug combinations with respect to potency and efficacy.

Christian T. Meyer[† 1,3], David J. Wooten[† 2,3], B. Bishal Paudel[† 4,5], Joshua Bauer[4,5,6], Keisha N. Hardeman[4,5], David Westover[6], Christine M. Lovly[5,7], Leonard A. Harris[3,4], Darren R. Tyson[3,4], and Vito Quaranta[* 3,4,8,9]

[1]Program in Chemical and Physical Biology, Vanderbilt University School of Medicine, Nashville, Tennessee.
[2]Program in Cancer Biology, Vanderbilt University School of Medicine, Nashville, Tennessee.
[3]Center for Cancer Systems Biology at Vanderbilt, Vanderbilt University, Nashville, Tennessee.
[4]Department of Biochemistry, Vanderbilt University Nashville, Tennessee.
[5]Vanderbilt Ingram Cancer Center, Vanderbilt University Medical Center, Nashville, Tennessee.
[6]Institute of Chemical Biology, High-Throughput Screening Facility, Vanderbilt University, Nashville, Tennessee.
[7]Department of Medicine, Division of Hematology and Oncology, Vanderbilt University Medical Center, Nashville, Tennessee.
[8]Department of Pharmacology, Vanderbilt University School of Medicine, Nashville, Tennessee.
[9]Lead Contact
[*]Correspondence should be directed to V.Q. (vito.quaranta@vanderbilt.edu).
[†]These authors contributed equally to this work.

Contents

1 Supplemental Figures

Figure S1: Phenomenological model underlying the Hill equation and corresponding extension to two drug case. Related to Figure 1. A) The Hill equation can be derived for a system of two states with characteristic effects ($E0$ and $E1$) for which the transition rate, and thereby the equilibrium, between the states is a function of the where d is the drug concentration and h represents the hill coefficient (also known as cooperativity). In our system, $E0$ and $E1$ are defined by the proliferation rate in minimal and maximal drug concentration (i.e. DIP Rate), represented by the slope of a log-transformed growth curve. Here, the case of an anti-proliferative drug is considered where $E1<0$ indicates maximal concentration of drug induces population regression and $E0>0$ indicating an untreated, expanding population. B) Allostery-inspired extension to a 4-state model of combination drug action used to derive the 2D generalization of the Hill equation. The equilibrium between the percent of cell affected by drug 1 or drug 2 alone ($A1$ and $A2$ respectively) and the doubly affected ($A12$) populations is governed by the concentration of drug 1 modulated by α_2 (which quantifies drug 2's action on the potency of drug 1) and by the converse, drug 2 multiplied by α_1. $E3$ represents the maximal effect of the combination. C) Combination surfaces with asymmetric synergistic potency ($\alpha_1>1$, $\alpha_2<1$). The three surfaces correspond to the following conditions (from left to right): combination with asymmetric potency and no synergistic efficacy ($E1=E2=E3$); combination with asymmetric synergistic potency with synergistic efficacy ($\min(E1,E2)>E3$); combination with asymmetric synergistic potency with antagonistic efficacy ($\min(E1,E2)<E3$).

Figure S2: Conflation of synergy of potency and efficacy in current synergy frameworks. Related to Figure 1. A) A survey of Loewe calculations on a range of hypothetical drug combinations across a DSD spanning synergistic to antagonistic potency and efficacy. For each combination of β and $\log(\alpha)$ (where $\alpha=\alpha_1=\alpha_2$), a corresponding value for Loewe synergy was calculated at the drugs' EC50, resulting in a contour map (see bar above DSD for color legend, white is effect sizes undefined by Loewe, i.e., the effect of the combination is greater than the maximum of either drug alone). Along the contour lines, Loewe synergy values remain the same, indicating conflation of synergistic potency and efficacy. As an example, Loewe calculations yield the same value for drug combinations X and O (0.5); whereas MuSyC reveals that combination X is synergistically potent, while combination O is synergistically efficacious. Complete dose-response surfaces for X and O are also shown to further clarify the resolution of synergistic potency and efficacy by MuSyC (Right panels). B-F) Synergy calculations for other methods show the same conflation of synergy of potency and efficacy. Bliss was also calculated at the combination of each drug at the EC50, otherwise synergy metrics are calculated using the whole surface. See STAR Methods section Quantification and Statistical Analysis for details on synergy calculations. G) Combination Index precludes synergy of efficacy by enforcing the maximum effect of the drug to equal 0. This assumption results in poor fits when Emax does not equal zero which is commonly observed experimentally (e.g., Figure 5E). H) The reduction in fit quality for Combination Index is a monotonically decreasing function of Emax for Emax>0. I-J) The equivalent dose model (Zimmer et al., 2016) also enforces an Emax of 0 resulting in a fit quality which decreases as Emax increases.

Figure S3: Bayesian synergy parameter estimation in the MuSyC algorithm. Related to STAR Methods. A) A particle swarm optimizer (PSO) was tested for convergence across several different data densities ranging from 5X5 to 25X25 grids. Within each density range, 25 different dose-response surfaces were fit (See STAR Methods section Quantification and Statistical Analysis, subsection Fitting Dose-Response Surfaces, for all parameters used). At all tested densities for all conditions, a minimum in the log-likelihood was observed after approximately 60 iterations. B) Comparison of the error in final fits of the parameters between three methods PSO alone followed by a non-linear least squares (NLLS) optimizer (Levenberg-Marquardt), Markov Chain Monte Carlo (MCMC) posterior estimation, and PSO seeded MCMC optimization. Y-axis is the L2-norm of the fitted parameters to the true parameters. Across all data densities, PSO seeded MCMC had the highest fit accuracy across different dose-response surface topologies. C) Synergy parameter uncertainty as a function of dose coverage. σ is the standard deviation of the MCMC trace. As the dose coverage decreases, there is a commensurate increase in the uncertainty of in the fit across different dose-response surfaces. D) Trace-plots and posterior distributions of $\log(\alpha_1)$, $\log(\alpha_2)$, and $E3$ for a surface where max dose is equal to the EC50 (bottom). Red line demarcates the true value. Middle plot is the z-score of 20 segments from the overall sample ordered by trace number. Parameters which have absolute z-scores >2 at any point in the trace are considered not to have converged. E) Trace-plots and posterior distributions of $\log(\alpha_1)$, $\log(\alpha_2)$, and $E3$

for a surface where max dose is 10,000 times the EC50 fully capturing the drug effect saturation. Posterior distributions are narrower than for the surface with less coverage corresponding to an increase in uncertainty. However, other factors than dose-selection can contribute to fit uncertainty including experimental noise, density of data, steepness of single drug curves (i.e., the hill coefficient), and quality of priors in the MCMC fit.

Figure S4: Synergistic potency (α_1, α_2) and efficacy (β) do not depend on the potency and efficacy of the single drugs (C and Emax) and are independent of one another. Related to Figure 2. A) Jitter plot of the 64 surveyed single drug's Emax(obs), C [uM], and hill slope h. B) Synergy parameters do not correlate (Pearson-r) with a single drug's potency and efficacy in isolation. (α_2=X potentiates osimertinib). C) α_1 is independent of α_2 in the NSCLC screen. α_1 vs. α_2 by drug class examining the potentiation of drug X by osimertinib (α_1) and the potentiation of osimertinib by drug X (α_2). Ceritinib is not potentiated by osimertinib (last panel) while osimertinib is potentiated by ceritinib (Figure 2C).

Figure S5: Synergistic potency, synergistic efficacy, and maximal effect of combined RAFi and MEKi. Related to Figure 3. A) Jitter plots of $\log(\alpha_1)$ for each RAFi for the 4 MEKi tested. α_1 corresponds to the alteration in MEKi's effective dose due to the presence of a RAFi. Dashed line denotes zero separating synergistic and antagonistic potency. The color of plotted points is corresponds to the cell line as annotated at the bottom of the figure. B) Jitter plots of $\log(\alpha_2)$ for each MEKi for the 4 RAFi tested. α_2 corresponds to the alteration in RAF inhibitor's effective dose due to the presence of a MEK inhibitor. C) Rank ordered jitter plots of the median βobs for each drug combination across all cell lines. D) Distribution of maximal effects for RAFi alone ($E1$, 4 drugs), MEKi alone ($E2$, 4 drugs), and the combination ($E3$, 16 combinations) for each cell line. Orange bar denotes mean.

Figure S6: Errors in Melanoma dataset for other methods. Related to Figure 5. Distribution of synergy calculated by Loewe, CI, and Bliss for melanoma dataset. As in the PC9 data, Loewe was calculated directly from DIP rates, while CI and Bliss were calculated from 72-hour viability. Conditions for which synergy is undefined were not included (See STAR Methods, Section Quantification and Statistical Analysis). By these traditional methods, combinations of BRAF/MEK inhibitors in melanoma are ambiguous, spanning synergy (Syn-gray) and antagonism (Ant-white). $\log(\alpha_1)$ is the RAFi's effect on the potency of the MEKi and $\log(\alpha_2)$ is the reverse. Abbreviations of the RAF inhibitors are: dab=dabrafenib, plx=plx4720, raf=raf265, and vem=vemurafenib.

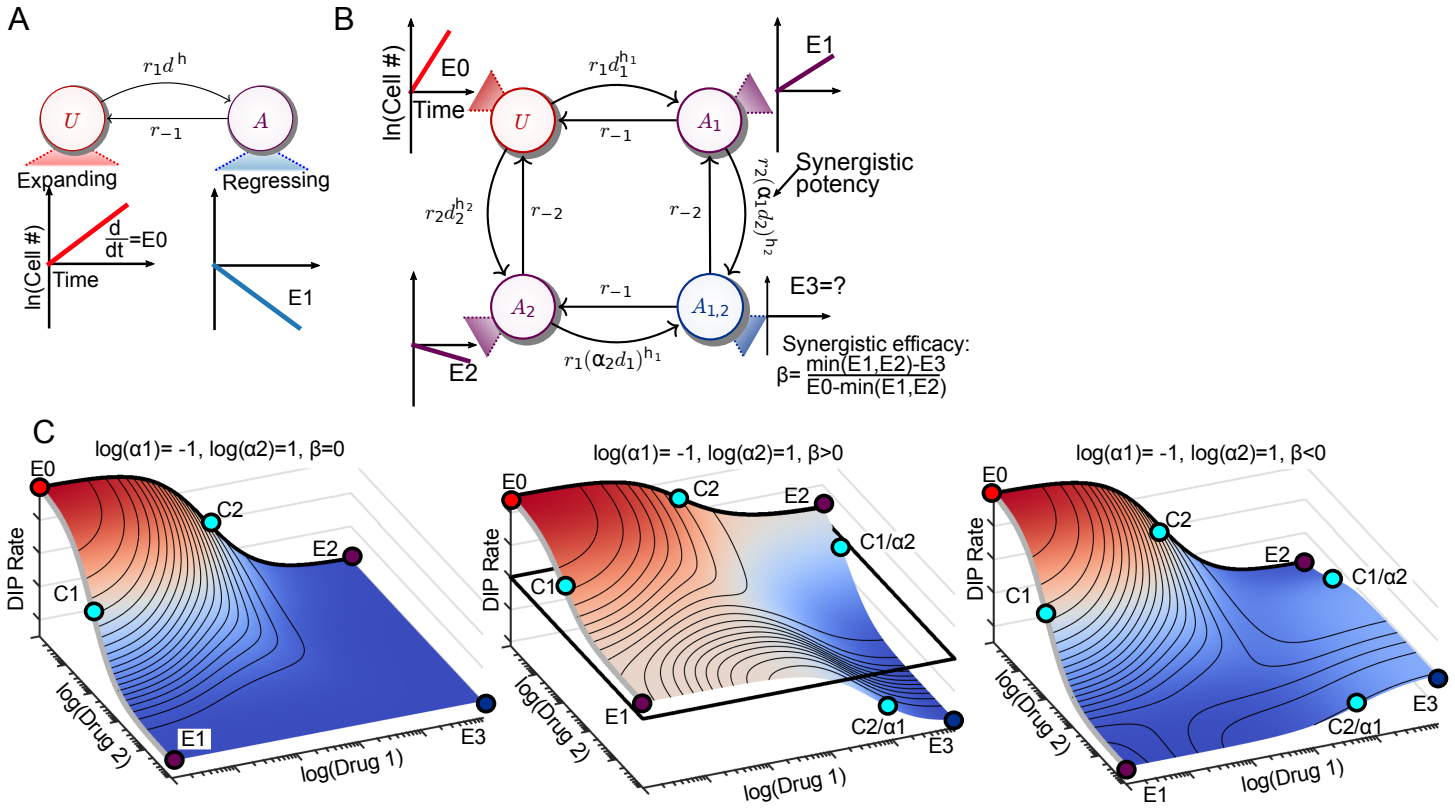
A
B
C
Expanding
Regressing
Time
E1
E0
E2
E3=?
Synergistic potency
Synergistic efficacy:
β= min(E1,E2)-E3 / E0-min(E1,E2)
log(α1)= -1, log(α2)=1, β=0
log(α1)= -1, log(α2)=1, β>0
log(α1)= -1, log(α2)=1, β<0
DIP Rate
log(Drug 1)
log(Drug 2)
C1
C2
C1/α2
C2/α1

Figure S1

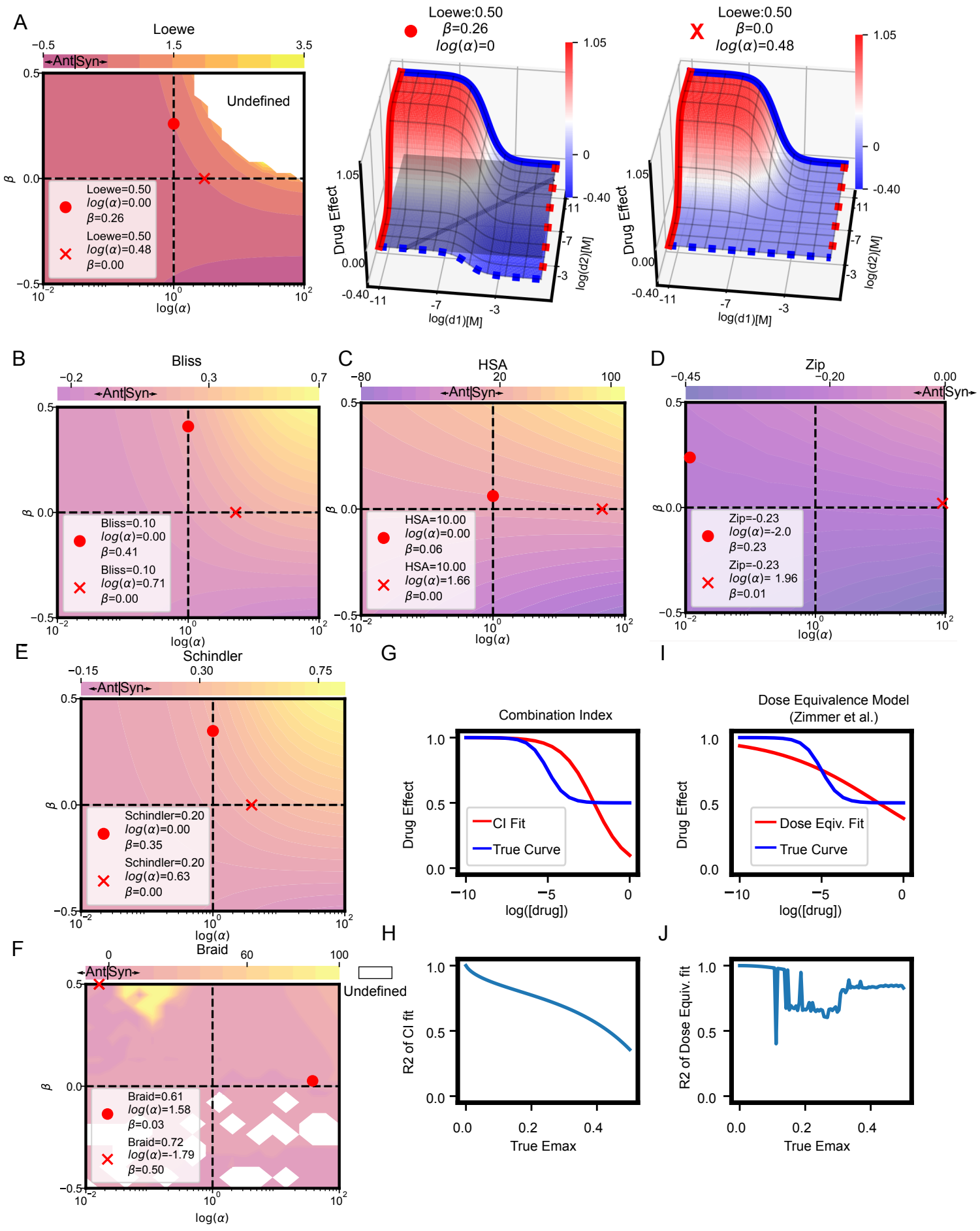
A
Loewe
Ant|Syn
Undefined
Loewe=0.50
log(α)=0.00
β=0.26
Loewe=0.50
log(α)=0.48
β=0.00
log(α)
β
Loewe:0.50
β=0.26
log(α)=0
Loewe:0.50
β=0.0
log(α)=0.48
Drug Effect
log(d1)[M]
log(d2)[M]
B
Bliss
Bliss=0.10
log(α)=0.00
β=0.41
Bliss=0.10
log(α)=0.71
β=0.00
C
HSA
HSA=10.00
log(α)=0.00
β=0.06
HSA=10.00
log(α)=1.66
β=0.00
D
Zip
Zip=-0.23
log(α)=-2.0
β=0.23
Zip=-0.23
log(α)= 1.96
β=0.01
E
Schindler
Schindler=0.20
log(α)=0.00
β=0.35
Schindler=0.20
log(α)=0.63
β=0.00
F
Braid
Undefined
Braid=0.61
log(α)=1.58
β=0.03
Braid=0.72
log(α)=-1.79
β=0.50
G
Combination Index
CI Fit
True Curve
log([drug])
I
Dose Equivalence Model
(Zimmer et al.)
Dose Eqiv. Fit
True Curve
H
R2 of CI fit
True Emax
J
R2 of Dose Equiv. fit
True Emax

Figure S2

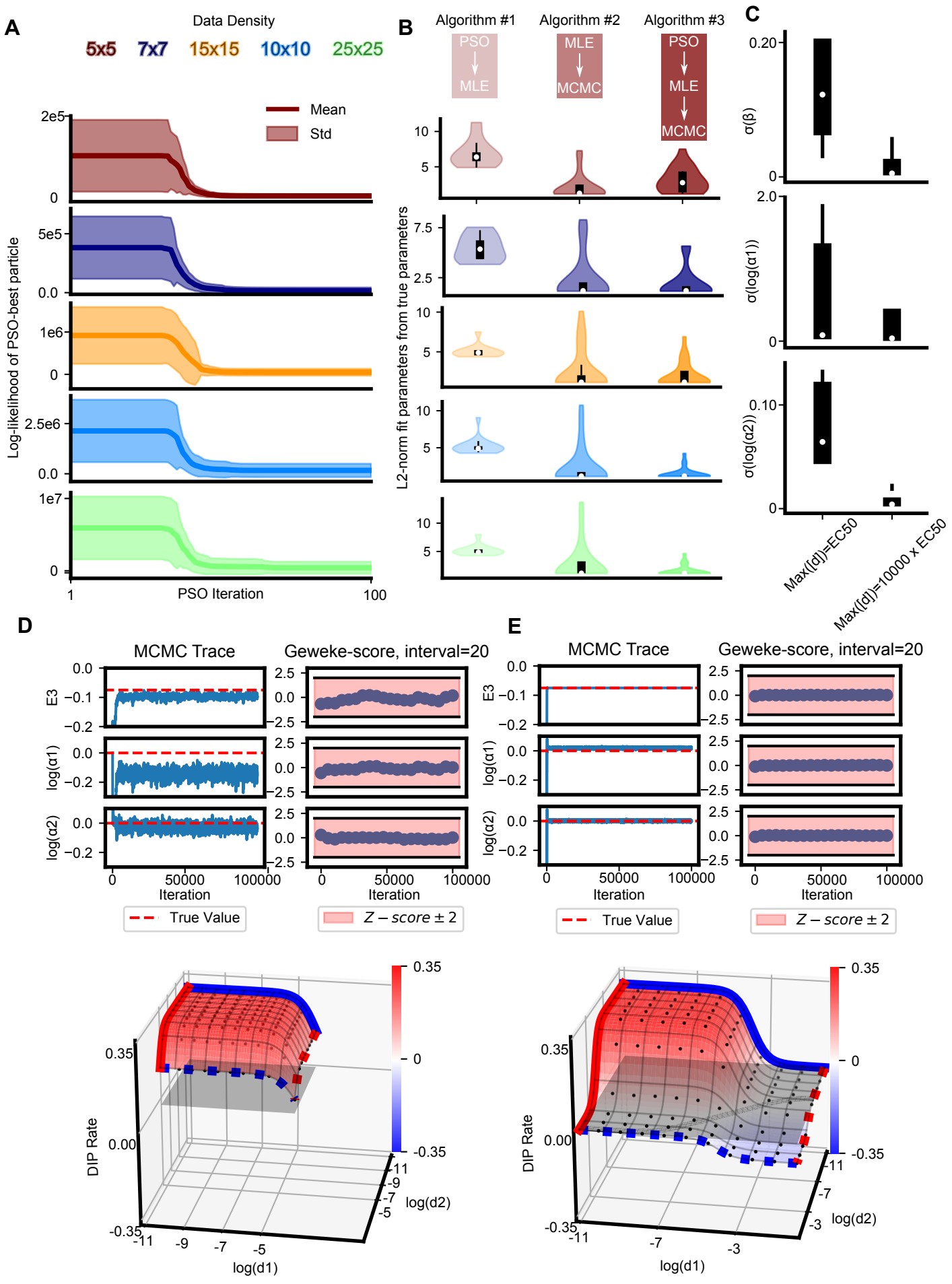
A
Data Density
5x5
7x7
15x15
10x10
25x25
Mean
Std
Log-likelihood of PSO-best particle
PSO Iteration
B
Algorithm #1
Algorithm #2
Algorithm #3
PSO
MLE
MCMC
L2-norm fit parameters from true parameters
C
σ(β)
σ(log(α1))
σ(log(α2))
Max(|d|)=EC50
Max(|d|)=10000 x EC50
D
MCMC Trace
Geweke-score, interval=20
E3
log(α1)
log(α2)
Iteration
True Value
Z – score ± 2
E
DIP Rate
log(d1)
log(d2)

Figure S3

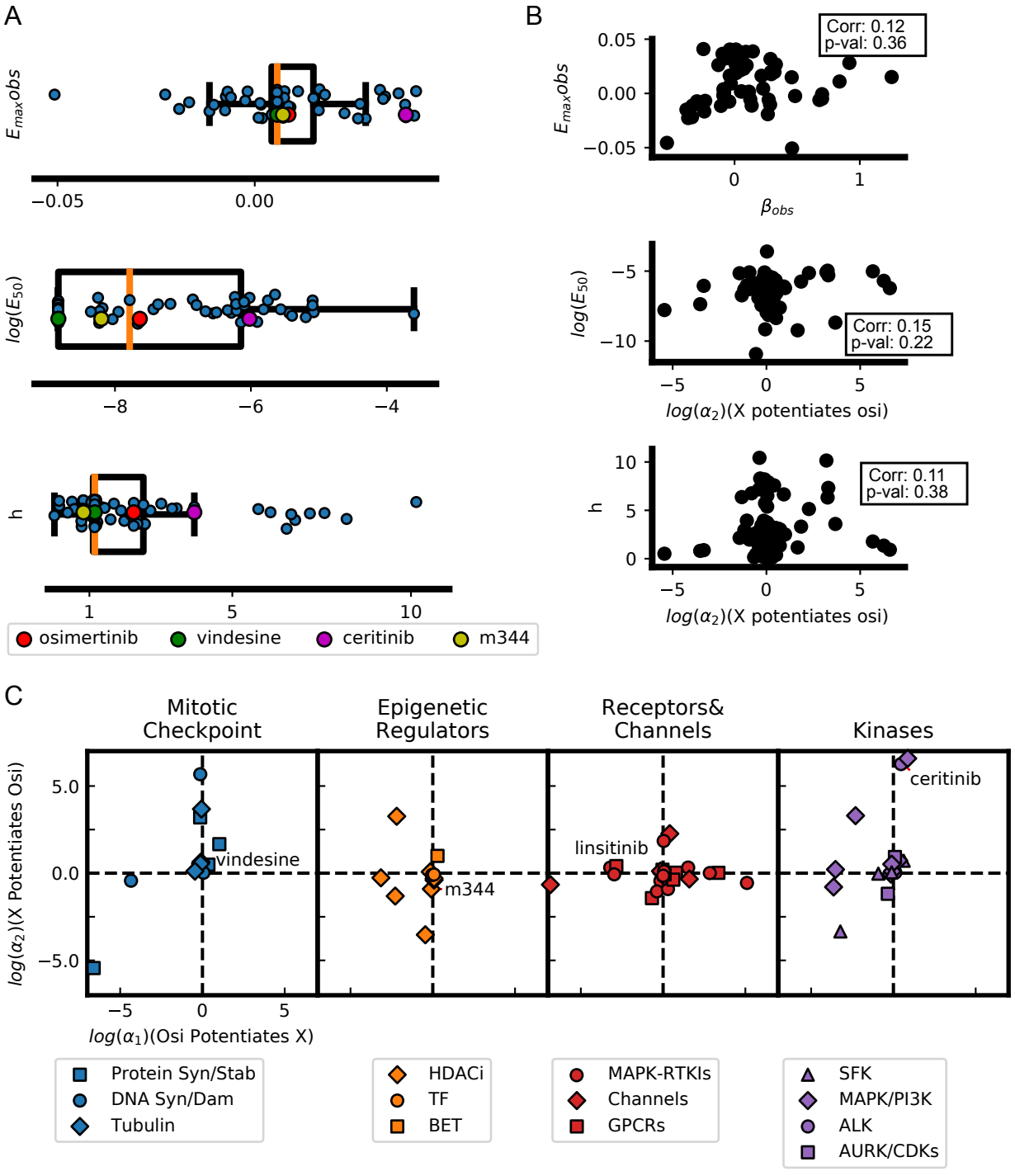
A
B
C
Corr: 0.12
p-val: 0.36
Corr: 0.15
p-val: 0.22
Corr: 0.11
p-val: 0.38
osimertinib
vindesine
ceritinib
m344
Mitotic Checkpoint
Epigenetic Regulators
Receptors& Channels
Kinases
vindesine
m344
linsitinib
ceritinib
Protein Syn/Stab
DNA Syn/Dam
Tubulin
HDACi
TF
BET
MAPK-RTKIs
Channels
GPCRs
SFK
MAPK/PI3K
ALK
AURK/CDKs

Figure S4

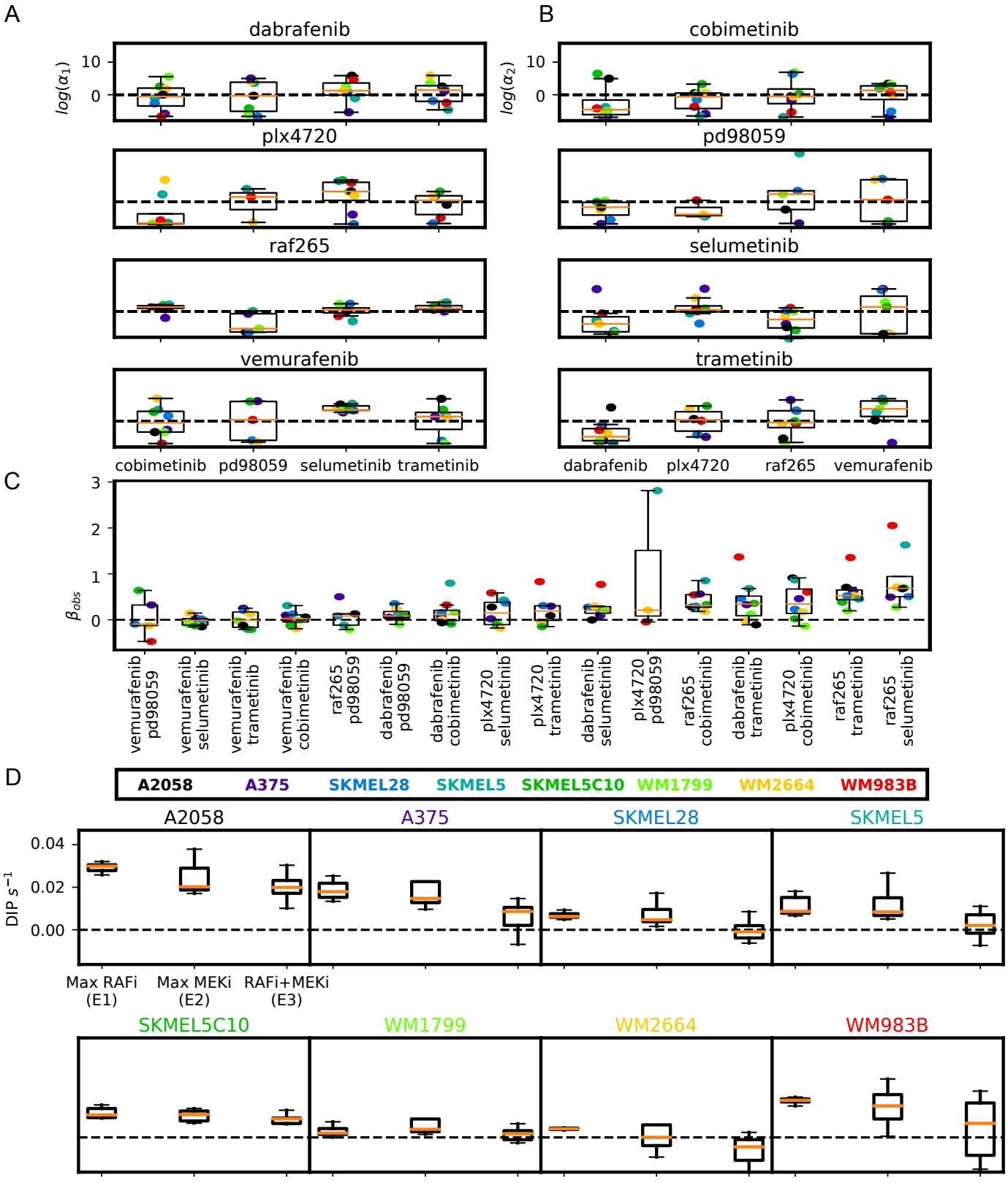
A
dabrafenib
plx4720
raf265
vemurafenib
$log(\alpha_1)$
10
0
cobimetinib
pd98059
selumetinib
trametinib
B
cobimetinib
pd98059
selumetinib
trametinib
$log(\alpha_2)$
dabrafenib
plx4720
raf265
vemurafenib
C
β_{obs}
3
2
1
0
vemurafenib pd98059
vemurafenib selumetinib
vemurafenib trametinib
vemurafenib cobimetinib
raf265 pd98059
dabrafenib pd98059
dabrafenib cobimetinib
plx4720 selumetinib
plx4720 trametinib
dabrafenib selumetinib
plx4720 pd98059
raf265 cobimetinib
dabrafenib trametinib
plx4720 cobimetinib
raf265 trametinib
raf265 selumetinib
D
A2058
A375
SKMEL28
SKMEL5
SKMEL5C10
WM1799
WM2664
WM983B
DIP s^{-1}
0.04
0.02
0.00
Max RAFi (E1)
Max MEKi (E2)
RAFi+MEKi (E3)

Figure S5

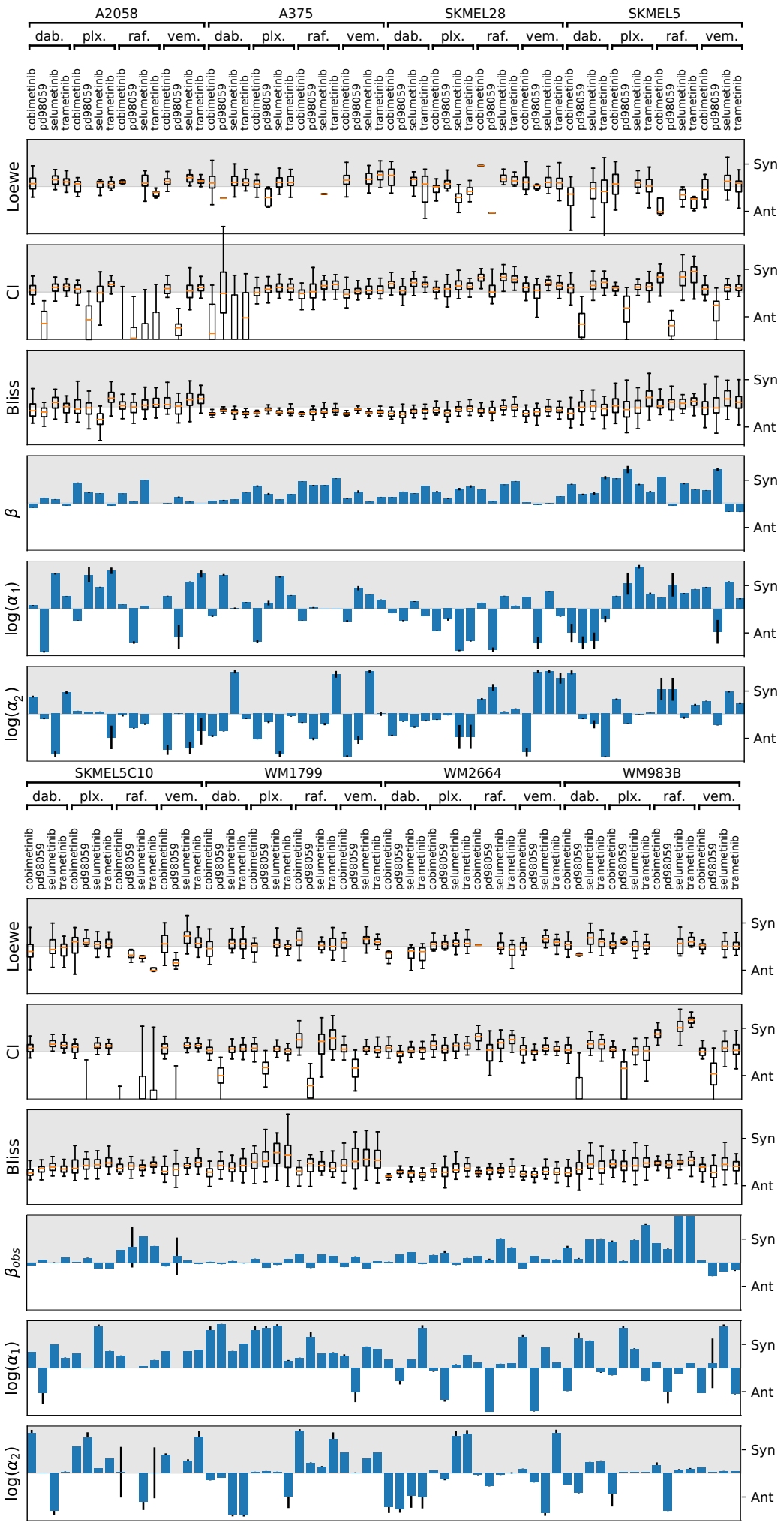
A2058
A375
SKMEL28
SKMEL5
dab.
plx.
raf.
vem.
cobimetinib
pd98059
selumetinib
trametinib
Loewe
CI
Bliss
β
log(α1)
log(α2)
Syn
Ant
SKMEL5C10
WM1799
WM2664
WM983B
βobs

Figure S6

2 Supplemental Tables

Table S1: Annotation of parameters for the 2D Hill equation. Related to Figure 1, Figure S1.

U	Percent of unaffected cells
A_1, A_2	Percent of cells affected by drug 1 and drug 2, respectively.
$A_{1,2}$	Percent of cells affected by both drug 1 and drug 2.
d_1, d_2	Drug concentrations for drug pair
E_d	Measured DIP rate at (d_1, d_2)
C_1,C_2	EC_{50} for drugs 1 and 2 in isolation
r_x, r_{-x}	The forward and reverse transition rates between two states
h_1,h_2	Hill coefficients for dose response curves of drug 1 and 2 in isolation
E_0	The basal rate of proliferation in drug naive condition
E_1,E_2	E_{max} of drug 1 and 2 in isolation
E_3	E_{max} of the combination of drugs 1 and 2
α_1	Measure of how $[d_1]$ modulates the effective dose of $[d_2]$.
α_2	Measure of how $[d_2]$ modulates the effective dose of $[d_1]$.
β	Theoretical difference in maximal effect achievable with both drugs compared to the most efficacious drug alone.
β_{obs}	Observed difference in effect with both drugs at the maximum tested concentration as compared to either drug alone.

Table S2: Annotation of anti-cancer drugs used in NSCLC and BRAF-mutant melanoma screens with nominal target and target class. Related to Figure 2,3.

Class	Subclass	Drug	Tested Range	Nominal Target
NSCLC				
Epigenetic Regulators	BET	jq1	4.0uM-0.1nM,0nM	BET bromo-domain
	HDACi	abexinostat	0.3uM-0.8nM,0nM	HDAC
		entinostat	1.0uM-2.6nM,0nM	HDAC
		givinostat	10.0uM-41.1nM,0nM	HDAC
		m344	1.0uM-2.6nM,0nM	HDAC
		mocetinostat	0.3uM-0.8nM,0nM	HDAC
		panobinostat	0.4uM-0.0nM,0nM	HDAC
		pracinostat	10.0uM-41.1nM,0nM	HDAC
		quisinostat	1.0uM-2.6nM,0nM	HDAC
	TF	bazedoxifene	10.0uM-41.1nM,0nM	ER
		verteporfin	10.0uM-41.1nM,0nM	YAP
Kinases	ALK	ceritinib	4.0uM-0.1nM,0nM	ALK/IGF1R
		ensartinib	4.0uM-0.1nM,0nM	ALK
	AURK/CDKs	bml259	1.0uM-2.6nM,0nM	CDK
		zm447439	4.0uM-0.1nM,0nM	AURK
	MAPK/PI3K	dactolisib	4.0uM-0.1nM,0nM	PI3K/mTOR
		ly294002	10.0uM-41.1nM,0nM	PI3K
		rapamycin	0.3uM-0.8nM,0nM	mTOR
		sb253226	10.0uM-41.1nM,0nM	p38
		tak632	4.0uM-0.1nM,0nM	RAF
		trametinib	0.3uM-0.8nM,0nM	MEK
		u0126	10.0uM-41.1nM,0nM	MEK
		ulixertinib	4.0uM-0.1nM,0nM	ERK
	SFK	bosutinib	10.0uM-41.1nM,0nM	Bcr-ABL/SFK
		dasatinib	1.0uM-3.9nM,0nM	SFK
		pp2	10.0uM-41.1nM,0nM	SFK
		quercetin	10.0uM-41.1nM,0nM	SFK
Mitotic Checkpoint	DNA Syn/Dam	carmustine	10.0uM-41.1nM,0nM	DNA
		methotrexate	4.0uM-0.1nM,0nM	DHFR
		olaparib	20.0uM-0.3nM,0nM	PARP
	Protein Syn/Stab	carfilzomib	4.0uM-0.1nM,0nM	Proteasome
		harringtonine	10.0uM-41.1nM,0nM	Ribosomes
		mg132	4.0uM-0.1nM,0nM	Proteasome
		tanespimycin	4.0uM-0.1nM,0nM	HSP90
	Tubulin	cephalomannine	10.0uM-41.1nM,0nM	Microtubules
		docetaxel	0.3uM-0.8nM,0nM	Microtubules
		vindesine	0.3uM-0.8nM,0nM	Microtubules
		vinorelbinetartrate	10.0uM-41.1nM,0nM	Microtubules
Receptors & Channels	Channels	amiodarone	10.0uM-41.1nM,0nM	NA Channels
		bendroflume-thiazide	1.0uM-2.6nM,0nM	Cl channel
		cabozantinib	4.0uM-0.1nM,0nM	C-Met/Axl/Ret
		dronedarone	10.0uM-41.1nM,0nM	NA Channels
		ivacaftor	10.0uM-41.1nM,0nM	CFTR
		nateglinide	1.0uM-2.6nM,0nM	ATP-dependent K channels

	GPCRs	acetylcysteine	10.0uM-41.1nM,0nM	Glutamate receptor
		aprepitant	10.0uM-41.1nM,0nM	Neuromedin receptor
		beclomethasonedipropionate	1.0uM-2.6nM,0nM	Glucocorticoid receptor
		loratadine	10.0uM-41.1nM,0nM	Histamine H1-receptors
		naftopidil	10.0uM-41.1nM,0nM	B1-adrenergic receptor
		nebivolol	10.0uM-41.1nM,0nM	B1 receptor
		sp600125	10.0uM-41.1nM,0nM	JNK
		thioridazine	10.0uM-41.1nM,0nM	Adrenergic receptor
	MAPK-RTKIs	afatinib	4.0uM-0.1nM,0nM	EGFR/HER2
		ag 879	1.0uM-2.6nM,0nM	HER2/RAF-1
		gefitinib	4.0uM-0.1nM,0nM	EGFR
		gsk1751853a	10.0uM-41.1nM,0nM	IGF1R/INSR
		gsk994854a	10.0uM-41.1nM,0nM	IGF1R/INSR
		gw458787a	10.0uM-41.1nM,0nM	EGFR/ERBB4
		gw644007x	10.0uM-41.1nM,0nM	Ret
		gw694590a	10.0uM-41.1nM,0nM	TIE2
		gw770249x	10.0uM-41.1nM,0nM	FLT3
		linsitinib	5.0uM-19.5nM,0nM	IGF1R
		ponatinib	4.0uM-0.1nM,0nM	FGFR
		tyrphostinag370	10.0uM-41.1nM,0nM	PDGFRbeta
BRAF-Mutant Melanoma				
Kinases	MAPK/PI3K	dabrafenib	0.4nM-0.39nM,0nM	BRAFV600
		plx4720	8.0uM-7.8nM,0nM	BRAFV600E & CRAF1
		raf265	1.0uM-3.9nM,0nM	CRAF,BRAF, & BRAFV600E
		vemurafenib	8.0uM-7.8nM,0nM	BRAFV600
		selumetinib	4.0uM-61pM,0nM	MEK1
		trametinib	0.4uM-6.1pM,0nM	MEK1/2
		pd98059	0.4uM-6.1pM,0nM	MEK1
		cobimetinib	0.8uM-12pM,0nM	MEK1

Table S3: BRAFi sensitivity across CCLE BRAF-mutant melanoma cell line panel. Related to Figure 3.

CCLE Cell Line	DIP Rate (h^{-1}) at [8uM] PLX4270
$A2058\_SKIN$	0.030
$A375\_SKIN$	0.005
$SKMEL28\_SKIN$	0.010
$SKMEL5\_SKIN$	0.014
$WM115\_SKIN$	0.013
$WM1799\_SKIN$	-0.002
$WM2664\_SKIN$	0.003
$WM793\_SKIN$	0.015
$WM88\_SKIN$	-0.020
$WM983B\_SKIN$	0.021

Table S4: Differentially Expressed Genes (DEGs) between SKMEL5 subclones SC01, SC07, SC10 whose expression significantly correlated to BRAFi insensitivity (Pearson r) across panel of 10 cell-lines (expression data from *Subramanian et al.*). See Table S3 for quantification of sensitivity to BRAFi. Related to Figure 3.

Positive Correlation with BRAFi insensitivity			Negative Correlation with BRAFi insensitivity		
Gene symbol	r	p-value	Gene symbol	r	p-value
SLC7A11	0.816	0.004	GRIK3	-0.743	0.014
SLC16A7	0.807	0.005	PRELP	-0.720	0.019
TGFB1	0.666	0.036	CPVL	-0.684	0.029
NOX5	0.649	0.042	ITGA10	-0.659	0.038
LXN	0.646	0.044			

Table S5: Description of nested model tiers used in MCMC fit. Related to STAR Methods.

Model Tier	Fit Parameters	Approximations
#5	α_1, α_2, E_3, E_1, E_2, C_1, C_2, h1, h2, E_0, r_1, r_2	1. Rate of transition (r1,r2) » 1.
#4	α_2, E_3, E_1, E_2, C_1, C_2, h1, h2, E_0	1. System obeys detail balance.
#3	α_2, E_3, E_1, E_2, C_1, C_2, h1, h2	1. All conditions tier 4 2. E0 is the minimally observed effect.
#2	α_2, E_3, E_1, E_2, C_1, C_2	1. All conditions tiers 3,4 2. h1,h2 are from single drug fits or 1 if single fits failed converge.
#1	α_2, E_3, E_1, E_2	1. All conditions tiers 2-4 2. C1,C2 are from single drug fits or the median concentrati if single fits failed to converge.
#0	α_2, E_3	1. All conditions tiers 1-4 2. E1, E2 are assumed to be the maximally observed effect maximum concentration of d1 and d2 respectively.